# A Machine Learning-Based Fault Identification and Classification Method for UPFC-Compensated Transmission Lines Integrated with Solar PV Systems

**Aniruddha Ray**
Department of Electrical Engineering, Agnel Charities Fr. C. Rodrigues Institute of Technology, Vashi, Navi Mumbai, Maharashtra, India
rayaniruddha24@gmail.com (corresponding author)

**S. Bindu**
Department of Electrical Engineering, Agnel Charities Fr. C. Rodrigues Institute of Technology, Vashi, Navi Mumbai, Maharashtra, India
bindu.s@fcrit.ac.in

*Received: 28 February 2026 | Revised: 7 April 2026 and 29 April 2026 | Accepted: 30 April 2026*

 *DOI: https://doi.org/10.48084/etasr.18435*

## ABSTRACT

**Unified Power Flow Controllers (UPFCs) are deployed to enhance transmission network performance, but can disrupt traditional distance protection, especially when integrated with solar power. This paper investigates the impact of a UPFC and a solar Photovoltaic (PV) plant on distance relay operation in a modified 39-bus New England test system, focusing on four fault types: single line-to-ground, line-to-line, double line-to-ground, and three-phase faults. The study finds that Zone-1 protection starts to malfunction under certain fault scenarios, including single line-to-ground and line-to-line faults with 40 Ω resistance, double line-to-ground with 10 Ω, and three-phase faults with 60 Ω. To address this, a Machine Learning (ML) approach is proposed for fault identification and classification. A dataset of 400 fault cases was generated by varying fault resistance, type, and location. The performance of four ML classifiers, Fine k-Nearest Neighbors (kNN), Linear Support Vector Machine (SVM), Bagged Trees, and Fine Decision Tree acting as a digital relay was analyzed using the dataset within the MATLAB Simulink environment. Linear SVM classifier achieved the highest performance, attaining 99.98% accuracy and 100% precision, 99.87% recall, and an F1-score of 0.9993 for the ABC fault; 99.78% precision, 100% recall, and an F1-score of 0.9989 for the C–G fault; and 100% precision, recall, and F1-score for the remaining fault scenarios while exhibiting a superior Receiver Operating Characteristic (ROC) curve. The trained SVM classifier identified the fault types correctly even with a 10 dB random noise.**

***Keywords-distance protection; UPFC; Solar Plants; New England 39 bus system; SVM; fault classification***

## I. INTRODUCTION

To address the growing electricity demand, power utilities are striving to make optimal use of existing transmission infrastructure [1]. One key strategy involves enhancing the capacity of transmission lines through the deployment of Flexible AC Transmission Systems (FACTS). Among the various FACTS technologies, the Unified Power Flow Controller (UPFC) is commonly implemented to regulate and improve power flow along transmission corridors. However, the inclusion of a UPFC in the fault path significantly alters the voltage and current signals observed at the relay location. As a result, traditional distance relays encounter difficulties in accurately detecting faults in UPFC-compensated lines. At the same time, the integration of utility-scale solar power plants into transmission networks is rapidly increasing, with installations reaching megawatt-level capacities [2]. When such systems are combined with FACTS compensation, particularly with UPFCs, the design and coordination of distance protection schemes become increasingly complex, requiring advanced solutions. Developments in power system protection have led researchers to explore innovative techniques that enhance the distance protection of transmission lines. One such contribution involves the use of the Intrinsic Time Decomposition method to identify faults in networks connected to utility-scale Photovoltaic (PV) systems [3]. Authors in [4] proposed a solution for protecting series-compensated parallel transmission paths supplying solar power, utilizing locally available positive sequence current and voltage data for fault

analysis. Authors in [5] calculated the phase angle of the fault loop current from local input signals to improve decision accuracy in the presence of converter-based energy sources. Authors in [6] introduced a data-mining method that employs a Convolutional Neural Network-based classifier to identify different fault types in a power system network. Authors in [7] introduced an intelligent protection mechanism based on a deep convolutional neural network for quickly identifying and classifying faults in UPFC-compensated transmission lines connected to large doubly-fed induction generator-based wind energy farms. Authors in [8] proposed a location estimation method for faults in double-circuit lines equipped with UPFC, based on synchronized measurements of negative sequence currents taken from both line ends. Authors in [9] presented a combined technique for identifying and locating asymmetrical faults in UPFC-compensated transmission infrastructure by utilizing time-synchronized voltage and current data from each end of the line. However, these research efforts have not emphasized improving the distance protection of UPFC compensated high voltage transmission lines integrated with inverter-based Solar PV Plants.

In this paper, the performance of the relay is evaluated in MATLAB by simulating four different fault types on a UPFC-Compensated Transmission Line Connecting the Solar Plant (UPFCTLSP). Four Machine Learning (ML) approaches are utilized for fault identification and classification for a UPFCTLSP. Among these, the Linear Support Vector Machine (SVM) algorithm is proposed, as it demonstrates superior performance compared to the other three techniques.

## II. SYSTEM DESCRIPTION

The IEEE 39-bus system is widely known as the 10-machine New England power grid. This benchmark network consists of 10 generating units along with 46 transmission lines [10]. Figure 1 presents a 345 kV, 60 Hz, 39-bus configuration of the modified New England power grid to address the challenges and explore mitigation strategies related to distance protection in the presence of a UPFC device and an integrated solar generation unit [11].

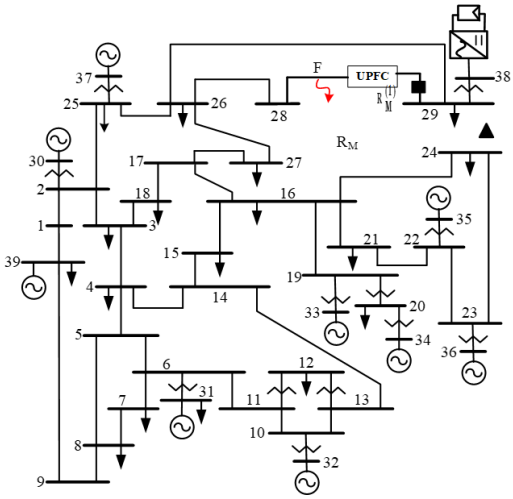


Fig. 1. New England 39-bus system with UPFC device and solar plant [11].

A UPFC is deployed at the sending terminal of line (29–28) and operates under the Automatic Power Flow Control mode [12]. Additionally, the conventional generator at Bus 29 is substituted with solar power generation rated at 1000 MW. The solar PV system operates near unity power factor, as stipulated by North American Grid Codes (NA-GCs) [13]. Incorporating the aforementioned modifications, the final test network is developed in MATLAB Simulink.

## III. PERFORMANCE ANALYSIS OF DISTANCE RELAY IN A UPFCTLSP

### A. *Computation of Boundary Points for the Quadrilateral Distance Relay Characteristics*

The quadrilateral characteristics typically employed in distance relays within a power grid, excluding the influence of the UPFC device and solar plant integration were taken from [14]. The coordinates outlining the quadrilateral relay characteristic are determined based on transmission line data of the New England 39-bus system, as illustrated in Figure 1. The Zone-I quadrilateral relay $R_M^{(1)}$ positioned at the sending end of the transmission line segment between buses 29 and 28 is designed to cover faults with resistance values up to 50 Ω.

For phase-to-ground faults, the computed coordinates for points A, B, C, E, and P are: A (–11.5641, 43.15792), B (53.99936, 43.15792), C (50, –13.3974), E (3.99936, 43.15792), and P (0, 0). These coordinate values are relevant for single line-to-ground (A-G) faults as well as double line-to-ground (B-C-G) fault conditions. For phase-to-phase faults, the calculated coordinates for points A, B, C, E, and P are: A (-3.85469, 14.38592), B (51.33312, 14.38592), C (50, –13.3974), E (1.33312, 14.38592), and P (0, 0). The computed coordinates are applicable to both line-to-line (B–C) faults and symmetrical three-phase (A–B–C) fault conditions.

Figure 2 shows the apparent impedance trajectory, which remains within the Zone-I boundary of the distance relay for a three-phase fault (ABC fault) with a fault resistance of 30 Ω at 70% of the length of the (29–28) transmission line, as displayed in Figure 1.

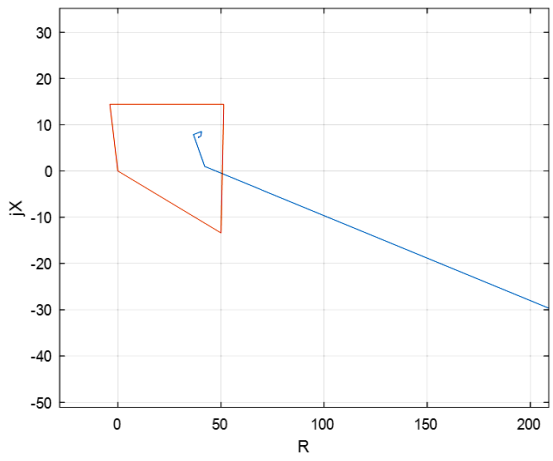


Fig. 2. Apparent impedance trajectory during a three-phase (ABC) fault with 30 Ω fault resistance, excluding the effect of the UPFC device and PV integration.

### *B. Performance of the Distance Relay in Modified 39 Bus Test System*

The performance of the conventional quadrilateral relay, designed as described above, is analyzed in the modified test system (Figure 1). To regulate the power flow according to predefined reference values, the UPFC control mechanism is activated at t = 7 s. The behavior of the distance relay is then evaluated by introducing various fault types at t = 9 s, occurring at 70% of the length of the (29–28) line segment measured from bus 29. A summary of the simulation outcomes for all tested cases is provided in Table I, which shows that the relay performance deteriorates at higher fault resistance levels, such as 50 Ω and 60 Ω, where it fails to detect any fault types. For example, Figures 3(a) and 3(b) show that the apparent impedance trajectories remain outside the Zone-I boundary for the following fault scenarios: a single line-to-ground fault and a line-to-line fault with a fault resistance of 40 Ω. This indicates that the relay fails to detect the fault within its protection zone.

### *C. Effect of the Solar Plant on the Apparent Impedance Seen by the Relay*

In contrast to synchronous generators, a solar power plant operates as a controlled current source [14]. The control scheme used in inverters restricts the current magnitude supplied by the plant and adjusts its phase angle according to the grid code requirements of the connected power system. Consequently, the impedance measured by the relay does not match the true positive-sequence impedance of the respective line section. Hence, the relay maloperates as it is not able to detect the fault in the first zone.

### *D. Effect of the UPFC Device on the Apparent Impedance Seen by the Relay*

When UPFC devices are included within the fault loop, their series voltage and shunt current injections will influence both steady state and transient portions of voltage and current waveforms [15]. Hence, the apparent impedance calculated by a conventional distance relay differs from that obtained in a network operating without UPFC compensation. As a result, the distance relay may underreach or overreach in response to faults that occur within its protection zone.

TABLE I. DISTANCE RELAY BEHAVIOUR UNDER VARIOUS FAULT SCENARIOS

| Sr. no. | Fault resistance | A-G fault | B-C fault | B-C-G fault | ABC fault |
|---|---|---|---|---|---|
| 1 | 1 Ω | Detects fault | Detects fault | Detects fault | Detects fault |
| 2 | 10 Ω | Detects fault | Detects fault | No fault detection | Detects fault |
| 3 | 20 Ω | Detects fault | Detects fault | No fault detection | Detects fault |
| 4 | 30 Ω | Detects fault | Detects fault | No fault detection | Detects fault |
| 5 | 40 Ω | No fault Detection | No fault detection | No fault detection | Detects fault |
| 6 | 50 Ω | No fault detection | No fault detection | No fault detection | Detects fault |
| 7 | 60 Ω | No fault detection | No fault detection | No fault detection | No fault detection |

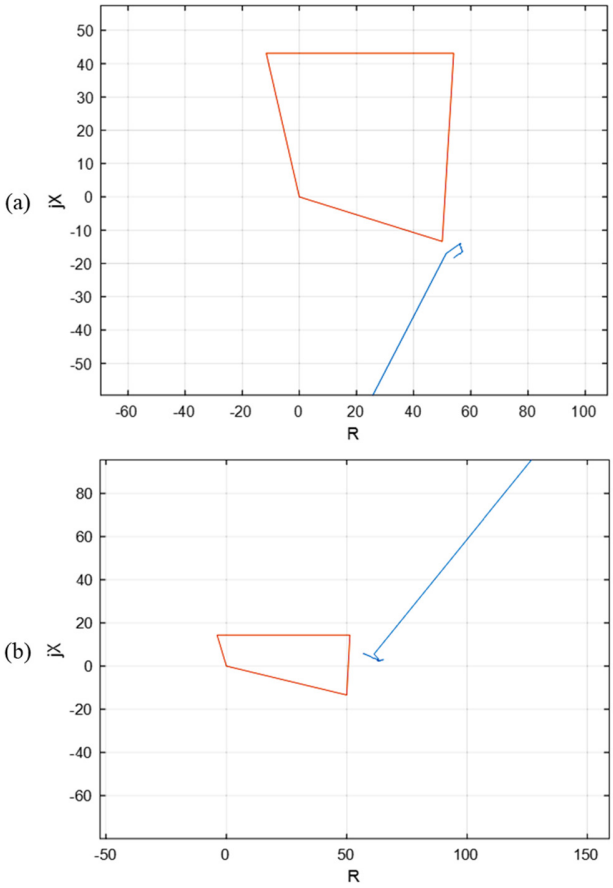


Fig. 3. Apparent impedance trajectory during: (a) single-line-to-ground (AG) fault with 40 Ω fault resistance, and (b) a line-to-line (BC) fault with 40 Ω fault resistance.

The integration of inverter-based PV power plants into UPFC-compensated transmission lines adds complexity to the performance of conventional distance protection schemes [16]. Therefore, there is a need for an alternate protection scheme to ensure the reliable operation of the relay in a UPFCTLSP.

## IV. FAULT IDENTIFICATION AND CLASSIFICATION METHODS

Fast and precise fault identification and classification are significant for ensuring effective protection of modern power systems [17]. To achieve this objective, ML–based techniques are used in numerical relays.

In this study, four ML algorithms, namely fine k-Nearest Neighbour (kNN), Linear SVM, Ensemble Bagged Trees, and Fine Decision Tree, are employed to identify and classify various fault types occurring in a UPFCTLSP [18]. The fine kNN algorithm classifies data by locating a small group of training samples closest to the input, using distance-based measures like the Euclidean metric. It determines the class by identifying the most frequent label among these nearby instances, making it well-suited for accurate classification in datasets with subtle distinctions. In the kNN algorithm, the value of k indicates the number of neighbors that needs to be considered. It is a user-defined parameter that is given as input

to the algorithm. Out of the considered data elements, the class that is predominant is considered the value of the class label to be assigned to the test data. The Linear SVM model separates data classes by finding the optimal hyperplane that maximizes the margin between data points of different classes in a linearly separable feature space. New data points are classified based on which side of the hyperplane they fall, enabling fast and effective classification with minimal computational complexity. The Ensemble Bagged Trees classifier operates by combining the predictions of multiple decision trees trained on different subsets of the data created through bootstrap sampling. Each tree votes on the classification outcome, and the final decision is made by majority voting, which enhances accuracy and reduces overfitting compared to a single decision tree. The Fine Decision Tree algorithm classifies data by recursively splitting the input feature space into smaller, more detailed regions using many decision nodes, resulting in a deep tree structure. This fine-grained approach allows for precise classification by capturing subtle patterns in the data.

## V. RESULTS AND DISCUSSION

To evaluate the effectiveness of the ML-based protection strategy, the modified New England 39-bus system, as illustrated in Figure 1, was simulated using MATLAB Simulink in Phasor mode to collect the dataset. A total of 400 distinct fault scenarios were created by varying key parameters within the power network. The simulated fault cases are generated by considering 10 different fault types, including AG, BG, CG, AB, BC, CA, AB-G, BC-G, CA-G, and ABC faults, varying fault location -specifically at 25%, 50%, 70% , and 80% of length of the transmission line (1 km) measured from the relay bus (Bus 29) and varying fault resistances across 10 levels (0.01 Ω, 1 Ω, 10 Ω, 20 Ω, 50 Ω, 100 Ω, 120 Ω, 150 Ω, 180 Ω, and 200 Ω) at each location [17]. For fault classification, input features such as the magnitudes and phase angles of phase voltages (Va, Vb, Vc), phase currents (Ia, Ib, Ic), and the apparent impedance measured at the relay bus (Zapp) are extracted from the simulation and exported to the MATLAB workspace.

Figure 4 presents a flowchart outlining the steps involved in implementing an ML algorithm for fault classification within MATLAB Simulink.

A comprehensive dataset is generated and recorded over the time interval from 0 to 9 s, which is labeled as normal condition, and from 9 to 9.07 s, labeled according to the corresponding fault type. In total, 19577 × 14 observations were recorded and stored in an Excel file. The dataset was imported into the Classification Learner App available under the MATLAB apps menu. All extracted features were selected as predictors, while the normal condition and fault label serve as the response variables. Within the app, 70% of the data were allocated for training and the remaining 30% for testing [19]. Four classification algorithms, including fine kNN (with k = 1), Linear SVM, Ensemble Bagged Trees, and Fine Decision Tree, were trained and tested using this dataset with five-fold cross-validation in the Classification Learner App, and were sorted in descending order of test accuracy percentage (Figure 5). It can be seen that the Linear SVM classifier demonstrates the highest average identification and classification accuracy, achieving 99.98%. Therefore, the Linear SVM model is proposed in this study for further analysis.

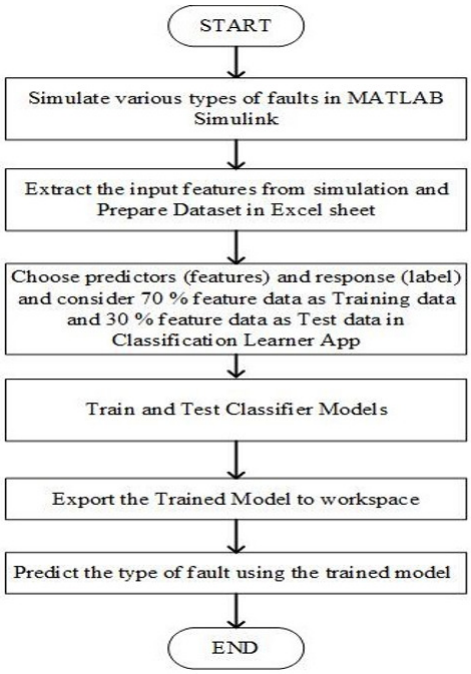


Fig. 4. Steps to implement an ML algorithm for fault classification in MATLAB Simulink.

The resulting test confusion matrix for the Linear SVM model is presented in Figure 6. This confusion matrix obtained in the Classification Learner app provides a summary of the classification performance of this Linear SVM model on a completely unseen test dataset, thus providing the final evaluation of the model's real-world ability. Based on the above test confusion matrix, performance metrics such as accuracy, recall, precision, and F1-score are computed separately for each fault type [20]:

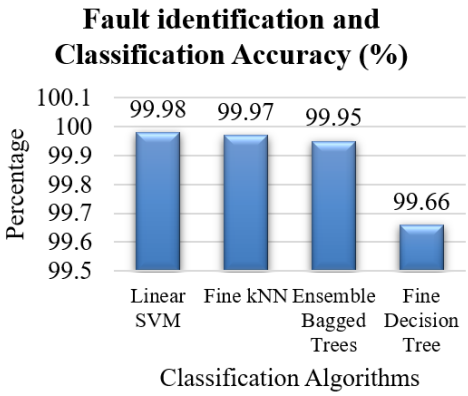


Fig. 5. Accuracy comparison of classification algorithms.

- Accuracy: The accuracy of each model was evaluated by:

$$\text{Accuracy} = \frac{(TP+TN)}{(TP+TN+FP+FN)} \quad (1)$$

where TP, TN, FP, and FN indicate the number of True Positives, True Negatives, False Positives, and False Negatives, respectively.

- Precision: The precision is defined as:

$$\text{Precision} = \frac{\text{TP}}{(\text{TP+FP})} \quad (2)$$

The precision for Class-1 (ABC fault) is found to be 100%.

- Recall: The recall is computed as:

$$\text{Recall} = \frac{\text{TP}}{(\text{TP+FN})} \quad (3)$$

The recall for Class-1 (ABC fault) is found to be 99.87%.

- F1-score: The F1-score is expressed as:

$$\text{F1 score} = \frac{(2 \times \text{Recall} \times \text{Precision})}{((\text{Recall+Precision}))} \quad (4)$$

The F1-score for Class-1 (ABC fault) is found to be 99.93%.

From the confusion matrix shown in Figure 6, it is observed that the FP and FN values are zero for the remaining classes. By using the above mathematical formula, the precision, recall, and F1-score of the remaining eight faults and the normal condition will all be 100%.

From the above results, it is found that the Linear SVM model achieves the highest accuracy, precision, recall, and F1-score for each fault; thereby, correctly detecting and classifying the normal condition and all 10 fault types, namely, A-G, B-G, C-G, AB, BC, CA, AB-G, BC-G, CA-G, and ABC faults.

- The Receiver Operating Characteristic (ROC) curve: Figure 7 illustrates the test ROC curves of the Linear SVM classifier for all classes. This model exhibits superior ROC performance for all classes as the curves pass through the point (0,1).

- The performance of the Linear SVM classifier in the presence of noise: a random noise with the following Signal to Noise Ratios (SNR) - 10 dB, 15 dB, 20 dB, and 25 dB is superimposed onto the current waveform, and the effectiveness of the proposed SVM approach is assessed [21]. For example, under noisy conditions, a single line-to-ground (A–G) fault is applied at 9 s, located at 70% of the transmission line length measured from the relay bus, with a fault resistance of 20 Ω. A test dataset consisting of 45×14 observations was generated and recorded over the time interval from 8.9 to 9.07 s for the above scenario, as depicted in Figure 8. The trained SVM classifier is exported to the MATLAB workspace, where it is utilized to identify fault types using the predict function, along with test data executed in the command window. In Figure 9, the results indicate that even with noise affecting the current, the trained SVM model classifies the fault type correctly.

The trained SVM model acts as a digital relay by extracting features from incoming signals. This classification output enables the relay to accurately identify the fault type and initiate appropriate protection actions. This intelligent, data-driven method significantly improves the accuracy and reliability of numerical relays under diverse fault scenarios.

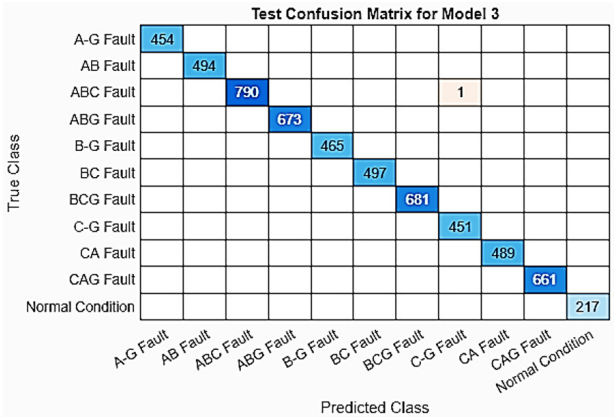


Fig. 6. Overall confusion matrix illustrating the performance of the Linear SVM classifier in fault identification and classification.

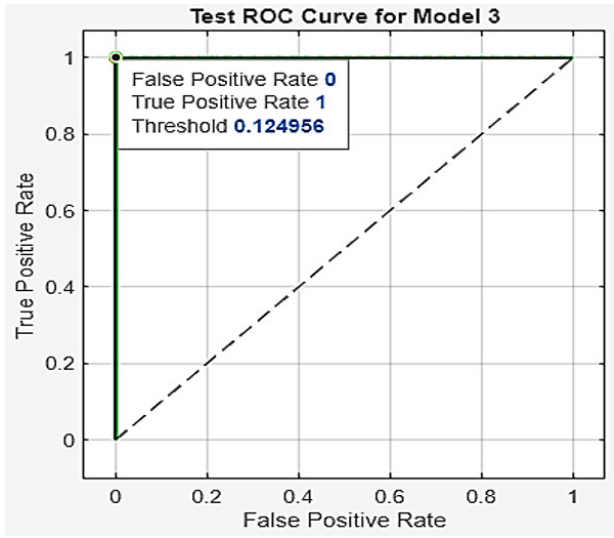


Fig. 7. ROC curve of Linear SVM classifier for all classes.

| Vamag | Vbmag | Vcmag | Vaangl | Vbangl | Vcangl | Iamag | Ibmag | Icmag | Iaangle | Ibangle | Icangle | Zappma | Zappangle |
|---|---|---|---|---|---|---|---|---|---|---|---|---|---|
| 269852 | 269851 | 269852 | -113.2 | 126.76 | 6.761 | 2300.3 | 732.62 | 943.94 | -38.48 | -134.1 | -8.106 | 62.287 | -72.54 |
| 269859 | 269857 | 269858 | -114.5 | 125.49 | 5.4904 | 2300.2 | 732.5 | 944.23 | -39.74 | -135.3 | -9.365 | 62.29 | -72.55 |
| 269868 | 269867 | 269868 | -115.8 | 124.22 | 4.2199 | 2300.3 | 733.03 | 943.55 | -41.01 | -136.6 | -10.62 | 62.291 | -72.55 |
| 269880 | 269879 | 269880 | -117.1 | 122.95 | 2.9497 | 2300.3 | 732.94 | 943.94 | -42.27 | -137.9 | -11.9 | 62.296 | -72.55 |
| 269895 | 269894 | 269895 | -118.3 | 121.68 | 1.6797 | 2300 | 732.67 | 944.09 | -43.55 | -139.1 | -13.16 | 62.301 | -72.55 |
| 269913 | 269912 | 269913 | -119.6 | 120.41 | 0.4101 | 2300.2 | 733.01 | 943.83 | -44.82 | -140.4 | -14.43 | 62.305 | -72.55 |
| 269934 | 269932 | 269934 | -120.9 | 119.14 | -0.859 | 2300.2 | 732.8 | 943.39 | -46.08 | -141.7 | -15.72 | 62.309 | -72.55 |
| 89657 | 239919 | 242703 | -142.4 | 134.49 | -16.15 | 2540.2 | 1100.5 | 555.4 | -112.9 | -154.3 | -30.86 | 18.536 | -28.12 |
| 89657 | 239919 | 242703 | -142.4 | 134.49 | -16.15 | 2540 | 1100.2 | 555.25 | -112.9 | -154.3 | -30.89 | 18.538 | -28.12 |
| 99154 | 233344 | 261380 | -151.3 | 134.87 | -14.43 | 2317.7 | 1103.8 | 466.64 | -121.2 | -158.8 | -27.14 | 22.403 | -28.35 |
| 97134 | 229397 | 256581 | -150.8 | 135.37 | -14 | 2319 | 1097.3 | 483.99 | -119.8 | -158.6 | -27.37 | 21.96 | -29.29 |
| 95773 | 230017 | 253282 | -151.8 | 136.02 | -14.17 | 2275.3 | 1085.8 | 487.75 | -119.3 | -158.9 | -26.14 | 22.096 | -30.65 |
| 94892 | 228862 | 254858 | -151.3 | 134.99 | -14.93 | 2284.2 | 1089.2 | 498.82 | -118.8 | -158.7 | -26.18 | 21.812 | -30.76 |
| 94795 | 226062 | 253840 | -152 | 135.05 | -14.77 | 2261.5 | 1087.3 | 502.21 | -119 | -159.2 | -25.62 | 22.021 | -31.27 |
| 93714 | 225846 | 252489 | -152.1 | 134.71 | -15.31 | 2254.7 | 1085.4 | 514.1 | -118.4 | -159.4 | -25.16 | 21.861 | -31.95 |
| 93326 | 223758 | 250754 | -152.6 | 134.43 | -15.5 | 2245.6 | 1085.4 | 526.63 | -118.3 | -160 | -24.73 | 21.891 | -32.54 |
| 92573 | 222432 | 248960 | -152.9 | 134.03 | -15.92 | 2246.5 | 1086.1 | 547.01 | -117.8 | -160.6 | -24.22 | 21.759 | -33.3 |
| 91821 | 220597 | 247113 | -153.4 | 133.72 | -16.26 | 2258.3 | 1088 | 577.62 | -117.4 | -161.7 | -23.94 | 21.548 | -34.34 |
| 91300 | 219402 | 245922 | -153.6 | 133.65 | -16.37 | 2289.7 | 1093.4 | 608.38 | -116.8 | -162.5 | -24.34 | 21.188 | -35.29 |
| 91222 | 219358 | 245973 | -153.6 | 133.88 | -16.17 | 2323.1 | 1099.7 | 623.11 | -116.2 | -162.5 | -25.43 | 20.855 | -35.81 |

Fig. 8. Snapshot of test dataset.

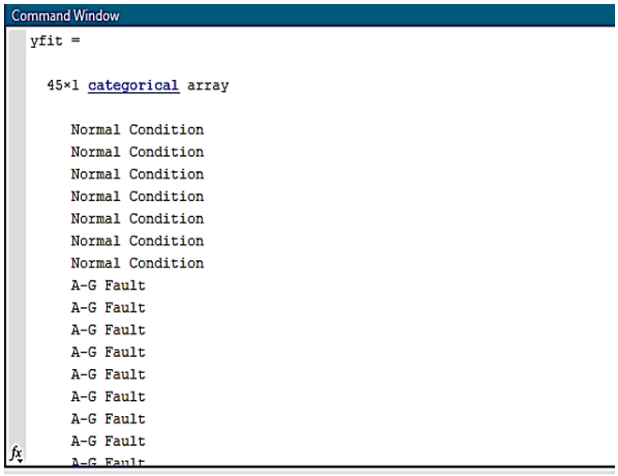


Fig. 9. Fault type identification using a trained SVM model in the MATLAB Command Window.

## VI. CONCLUSION

This paper investigates the performance of a distance relay in a Unified Power Flow Controller Compensated Transmission Line Connecting the Solar Plant (UPFCTLSP) under various fault conditions, including single line-to-ground, line-to-line, double line-to-ground, and three-phase faults. The conventional distance relay starts maloperating for all fault scenarios at a particular value of fault resistance. The apparent impedance observed by the relay under these conditions differs from the actual positive sequence line impedance between the relay point and the fault location due to the influence of shunt current injected by the shunt converter, the series voltage contribution from the series converter of the UPFC, and the fault current limitation imposed by the interfacing converters of the solar plant. To address this issue, a Machine Learning (ML)-based fault identification and classification method is proposed. Four ML classification algorithms were compared: Fine k-Nearest Neighbor (kNN), Linear Support Vector Machine (SVM), Ensemble Bagged Trees, and Fine Decision Tree. Out of the four classifiers, the Linear SVM model demonstrates the best overall classification performance. It achieved 99.98% accuracy. Furthermore, it exhibits a perfect Receiver Operating Characteristic (ROC) curve for each fault type in comparison with the other methods. Consequently, the trained SVM model was utilized to predict the type of fault using the test inputs through the MATLAB command window. Even with a 10 dB noise superimposed onto the current signal, the trained SVM model classifies the fault type correctly. Thus, the trained SVM model acts as a digital relay by identifying the fault type accurately and initiating appropriate protection actions. However, the effectiveness of this ML technique for fault identification and classification is highly dependent on the training dataset. Thus, this algorithm can ensure correct relay operation as long as the power system topology remains unchanged.

The high accuracy of all tested classifiers may be attributed to the noiseless training set and the low intensity (10 dB) test dataset. Future work will consider enhanced noise levels and real-life scenarios that may diversify the results.

## DECLARATION OF COMPETING INTERESTS

Not applicable to this work.

## ACKNOWLEDGMENT

Not applicable to this work.

## DATA AVAILABILITY

Not applicable to this work.

## REFERENCES

[1] S. Biswas and P. K. Nayak, "State-of-the-art on the protection of FACTS compensated high-voltage transmission lines: a review," *High Voltage*, vol. 3, no. 1, pp. 21–30, 2018, https://doi.org/10.1049/hve.2017.0131.

[2] V. Telukunta, J. Pradhan, A. Agrawal, M. Singh, and S. G. Srivani, "Protection challenges under bulk penetration of renewable energy resources in power systems: A review," *CSEE Journal of Power and Energy Systems*, vol. 3, no. 4, pp. 365–379, Dec. 2017, https://doi.org/10.17775/CSEEJPES.2017.00030.

[3] A. Jodaei, Z. Moravej, and M. Pazoki, "Effective protection scheme for transmission lines connected to large scale photovoltaic power plants," *Electric Power Systems Research*, vol. 228, Mar. 2024, Art. no. 110103, https://doi.org/10.1016/j.epsr.2023.110103.

[4] A. Chowdhury, S. Paladhi, and A. K. Pradhan, "Local positive sequence component based protection of series compensated parallel lines connecting solar photovoltaic plants," *Electric Power Systems Research*, vol. 225, Dec. 2023, Art. no. 109811, https://doi.org/10.1016/j.epsr.2023.109811.

[5] S. Paladhi, J. R. Kurre, and A. K. Pradhan, "Source-Independent Zone-1 Protection for Converter-Dominated Power Networks," *IEEE Transactions on Power Delivery*, vol. 39, no. 1, pp. 341–351, Feb. 2024, https://doi.org/10.1109/TPWRD.2022.3218615.

[6] M. Kiruthika and S. Bindu, "Classification of Electrical Power System Conditions with Convolutional Neural Networks," *Engineering, Technology & Applied Science Research*, vol. 10, no. 3, pp. 5759–5768, June 2020, https://doi.org/10.48084/etasr.3512.

[7] S. Biswas, P. K. Nayak, B. K. Panigrahi, and G. Pradhan, "An intelligent fault detection and classification technique based on variational mode decomposition-CNN for transmission lines installed with UPFC and wind farm," *Electric Power Systems Research*, vol. 223, Oct. 2023, Art. no. 109526, https://doi.org/10.1016/j.epsr.2023.109526.

[8] M. K. (Mondal) and S. Debnath, "Fault location in UPFC compensated double circuit transmission line using negative sequence current phasors," *Electric Power Systems Research*, vol. 184, July 2020, Art. no. 106347, https://doi.org/10.1016/j.epsr.2020.106347.

[9] B. Chatterjee and S. Debnath, "Sequence component based approach for fault discrimination and fault location estimation in UPFC compensated transmission line," *Electric Power Systems Research*, vol. 180, Mar. 2020, Art. no. 106155, https://doi.org/10.1016/j.epsr.2019.106155.

[10] I. Hiskens, "IEEE PES Task Force on Benchmark Systems for Stability Controls," Nov. 2013.

[11] A. Chowdhury, S. Paladhi, and A. K. Pradhan, "Adaptive Unit Protection for Lines Connecting Large Solar Plants Using Incremental Current Ratio," *IEEE Systems Journal*, vol. 16, no. 2, pp. 3272–3283, June 2022, https://doi.org/10.1109/JSYST.2021.3107331.

[12] K. Seethalekshmi, S. N. Singh, and S. C. Srivastava, "Synchrophasor Assisted Adaptive Reach Setting of Distance Relays in Presence of UPFC," *IEEE Systems Journal*, vol. 5, no. 3, pp. 396–405, Sept. 2011, https://doi.org/10.1109/JSYST.2011.2158694.

[13] S. Paladhi and A. K. Pradhan, "Adaptive Distance Protection for Lines Connecting Converter-Interfaced Renewable Plants," *IEEE Journal of Emerging and Selected Topics in Power Electronics*, vol. 9, no. 6, pp. 7088–7098, Dec. 2021, https://doi.org/10.1109/JESTPE.2020.3000276.

[14] A. Ray and S. Bindu, "Issues and Solution of Distance Protection of Grid Integrated with Solar PV plants," in *IEEE 2nd International Conference on Industrial Electronics: Developments & Applications*

(*ICIDeA*), Imphal, India, Sept. 29–30, 2023, pp. 229–234, https://doi.org/10.1109/ICIDeA59866.2023.10295210.

[15] X. Zhou, H. Wang, R. K. Aggarwal, and P. Beaumont, "Performance evaluation of a distance relay as applied to a transmission system with UPFC," *IEEE Transactions on Power Delivery*, vol. 21, no. 3, pp. 1137–1147, July 2006, https://doi.org/10.1109/TPWRD.2005.861329.

[16] A. Ray and Bindu. S., "Performance Assessment of Distance Protection in UPFC-Compensated Transmission Networks with Integrated Converter-Interfaced Renewable Energy Plants," in *2024 IEEE 1st International Conference on Green Industrial Electronics and Sustainable Technologies* (*GIEST*), Imphal, India, Oct. 25–26, 2024, pp. 1–6, https://doi.org/10.1109/GIEST62955.2024.10959819.

[17] S. K. Mohanty, S. Mohapatra, and M. Ramana, "Novel Protection Scheme For UPFC Compensated Line," in *2023 10th IEEE International Conference on Power Systems* (*ICPS*), Cox's Bazar, Bangladesh, Dec. 13–15, 2023, pp. 1–5, https://doi.org/10.1109/ICPS60393.2023.10428915.

[18] Saikat Dutt, Subramanian Chandramouli and Amit Kumar Das, *Machine Learning*. Pearson, 2018.

[19] S. Biswas, P. K. Nayak, and G. Pradhan, "A Transient-Extracting Transform Assisted Intelligent Fault Detection and Classification Approach for UPFC Installed Transmission Line," in *2022 IEEE IAS Global Conference on Emerging Technologies* (*GlobConET*), Arad, Romania, May 20–22, 2022, pp. 249–254, https://doi.org/10.1109/GlobConET53749.2022.9872493.

[20] S. Singh and P. K. Nayak, "Protection of high voltage transmission line connected large scale solar photovoltaic plant using green anaconda optimized machine learning method," *Computers and Electrical Engineering*, vol. 127, Oct. 2025, Art. no. 110618, https://doi.org/10.1016/j.compeleceng.2025.110618.

[21] S. Singh and P. K. Nayak, "A protection scheme for the transmission line connecting large-scale centralized solar PV plant," *Microsystem Technologies*, vol. 31, no. 7, pp. 1785–1805, 2025, https://doi.org/10.1007/s00542-024-05780-2.